Weierstraß-Institut
für Angewandte Analysis und Stochastik

im Forschungsverbund Berlin e.V.

Preprint ISSN 0946 – 8633

Numerical cooling strategy design for hot rolled dual phase steel

Piyada Suwanpinij[1], Nataliya Togobytska[2], Ulrich Prahl[1], Wolf Weiss[2], Dietmar Hömberg[2], Wolfgang Bleck[1]

submitted: April 20, 2010

[1] Department of Ferrous Metallurgy (IEHK)
RWTH Aachen University
Intzestr. 1
52072 Aachen
Germany
E-Mail: piyada.suwanpinij@iehk-rwth-aachen.de
ulrich.prahl@iehk.rwth-aachen.de
wolfgang.bleck@iehk.rwth-aachen.de

[2] Weierstrass Institute
for Applied Analysis and Stochastics
Mohrenstrasse 39
10117 Berlin
Germany
E-Mail: nataliya.togobytska@wias-berlin.de
wolf.weiss@wias-berlin.de
dietmar.hoemberg@wias-berlin.de

No. 1507
Berlin 2010

2000 *Mathematics Subject Classification.* 74N15, 34A55, 49N45.

Key words and phrases. Dual phase steel, hot rolling, process simulation, phase transformation, rate law model, parameter identification, process design.

This work is a part of the project "Simulation, Optimisation and Control of Microstructure Evolution and Mechanical Properties during Hot Rolling of Multiphase Steels" in the framework of SPP 1204 "Algorithms for fast material-specific process chain design and analysis in metal forming" funding by DFG (Deutsche Forschungsgemeinschaft).

Edited by
Weierstraß-Institut für Angewandte Analysis und Stochastik (WIAS)
Mohrenstraße 39
10117 Berlin
Germany

Fax: + 49 30 2044975
E-Mail: preprint@wias-berlin.de
World Wide Web: http://www.wias-berlin.de/

Abstract

In this article, the Mo-Mn dual phase steel and its process parameters in hot rolling are discussed. The process window was derived by combining the experimental work in a hot deformation dilatometer and numerical calculation of process parameters using rate law models for ferrite and martensite transformation. The ferrite formation model is based on the Leblond and Devaux approach while martensite formation is based on the Koistinen-Marburger (K-M) formula. The carbon enrichment during ferrite formation is taken into account for the following martensite formation. After the completion of the parameter identification for the rate law model, the evolution of phases in multiphase steel can be addressed. Particularly, the simulations allow for predicting the preferable degree of retained strain and holding temperature on the run out table (ROT) for the required ferrite fraction.

Introduction

Dual Phase steels (DP steels) have shown high potential for automotive applications due to their remarkable property combination with high strength and good formability [1]. The hot rolling process as illustrated in **Figure 1** has been proven to offer economical benefit for the production of DP steel as it provides good microstructure homogeneity with acceptable surface quality for many applications.

The hot rolling process of dual phase steel consists of 4 steps as shown in **Figure 1:**

1. Rolling in roughing and finishing stands, which results in the refinement of austenite grain size due to the repeating static recrystallisation,
2. Laminar cooling into two phase region,
3. Isothermal holding at ferrite transformation region temperatures, where the temperatures remain relatively constant,
4. Fast continuous cooling to the required coiling temperature, during which martensite transformation takes place and bainite transformation can be avoided.

The process window in hot rolling of dual phase steel is shown to be tight as only very short time in order of less than 10 s is allowed on the run out table (ROT) according to its limited length. An appropriate algorithm for the online control of the process parameters such as the time and temperature on ROT as well as the cooling rate during cooling down to coiling (step 4 in **Figure 1** is desirable indeed. An initial step towards this goal, the modelling and simulation of the evolution of phases on ROT will be discussed in this paper. The resulting model consists of two rate laws to predict the phase transformation in multiphase steels taking into account different process parameters such as austenite conditioning, holding time, temperature on ROT, and the following cooling rate to coiling temperature.

Initially, the process window was suggested by means of experiments in deformation dilatometer, whose results contributed to the parameter identification of the ferrite transformation model in terms of the effect of retained strain. After parameter identification the model is able to predict the resulting microstructure according to given process parameters and temperature profile. The results from process simulation in deformation dilatometer were then utilised to evaluate the simulation results.

The current work employed a Mo-Mn dual phase steel containing 0.08 wt-% C, 1.44 wt-% Mn, 0.15 wt-% Mo, 0.03 wt-% Si, 0.05 wt-% Al. The transformation kinetics show sufficient sensitivity to the process parameters mentioned above. It is therefore beneficial for the study and validation of the proposed numerical model.

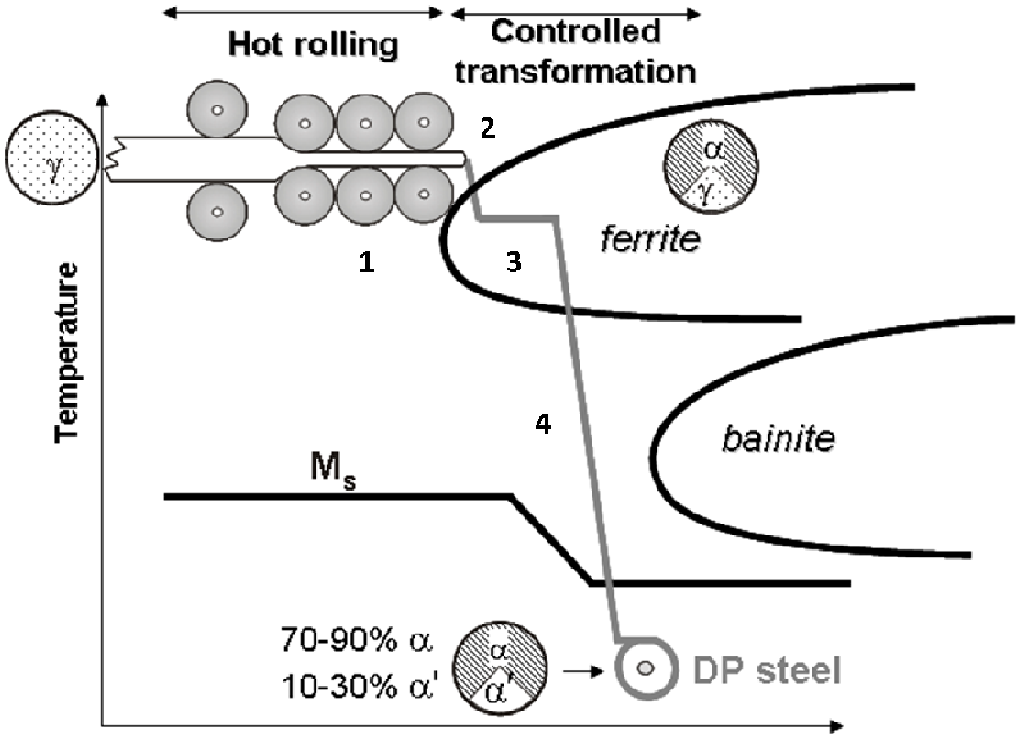

Figure 1: A **s**ketch of the processing scheme for hot rolled dual phase steel.

Rate law transformation model for hot rolled dual phase steels

The kinetics of phase transformations in steel can be described by a system of ordinary differential equations (ODEs). Details about the model can be found in [2]. In this paper the focus is on the formation of ferrite and martensite. In the sequel, their volume fractions will be denoted by *f* and *m*, respectively. Moreover, *T* is the temperature with time derivative $\dot{T}$. With these notations the growth of ferrite and martensite in hot rolled dual phase steel can be described by the system

$$\dot{f}(t) = \left[f_{eq} - f\right]_+ \cdot g_{f1}(T) \cdot g_{f2}(D_\gamma, \varepsilon) \tag{1}$$

$$\dot{m}(t) = \frac{1}{\tau_m}\left[\overline{m}(T, C_\gamma) - m\right]_+ \tag{2}$$

$$f(0) = m(0) = 0. \tag{3}$$

The expression $[u]_+$ in the model equations describes the positive part of a value *u*, i.e. $[u]_+ = \max\{u,0\}$. The term f_{eq} describes the asymptotic equilibrium fraction of ferrite as a function of temperature *T* after isothermal holding. It can be identified utilizing isothermal dilatometric experiments from a homogenised austenite state. The function $g_{f1}(T)$ relates to the isothermal transformation behaviour of ferrite, starting from homogeneous austenite state. The function $g_{f2}(D_\gamma,\varepsilon)$ couples the influence of austenite grain size D_γ and the effect of retained strain ε on the isothermal ferrite transformation kinetics.
The growth of martensite is described by a variant of the Koistenen-Marburger formula. Assuming that at any time *t* the maximal volume fraction of martensite that can be produced corresponds to the remaining volume fraction of austenite, i.e., $1-f$, the function $\bar{m}$ is defined by

$$\bar{m}(T,C_\gamma) = \min\{m_{KM}(T),1-f\}.$$

Here, m_{KM} describes the volume fraction of martensite according to the Koistinen and Marburger formula [3], i.e.,

$$m_{KM}(T,C_\gamma) = 1-e^{-c_{km}(M_s(C_\gamma)-T)}. \qquad (4)$$

C_γ is the carbon content in the remaining austenite after the ferrite transformation, which is increased due to carbon enrichment. An easy way to take care of carbon partitioning between ferrite and austenite is to define C_γ by

$$C_\gamma = \frac{C_{total}-C_f\cdot f}{1-f}$$

where C_{total} corresponds to the nominal carbon content of the respective steel, and C_f is the carbon content in ferrite, which can be computed from the empirical formula

$$C_f = 2.55\cdot e^{-\frac{4850}{T(K)}}.$$

Then, M_S as a function of C_γ can be calculated from [4]:

$$M_s(C_\gamma) = 506.6-338.7(C_\gamma)-18.3(Mn)+1.3(Si)-14.5(Cr). \qquad (5)$$

The coefficient c_{km} can be drawn from the respective dilatometric data.
The effect of austenite conditioning in step 1 of **Figure 1** is contained in the function $g_{f2}(D_\gamma,\varepsilon)$, which has the following form:

$$g_{f2}(D_\gamma,\varepsilon) = \alpha_1 S_v(D_\gamma,\varepsilon)+\alpha_2.$$

Here α_1,α_2 are the parameters that have to be fitted to the experimental data and the function S_v describes the effect of austenite grain size and retained strain. Due to the difficulty in defining S_v by experiment as the prior austenite grain boundaries are severely obscured by bainitic transformation during quenching deformed samples, S_v was taken from the empirical equation from Kvackaj [6] as shown in Eq. (6) and illustrated in **Figure 2**

$$S_v = 429\frac{1}{D_\gamma e^{\varepsilon}}+1571\frac{e^{\varepsilon}}{D_\gamma}+\left[157.2(1-e^{-\varepsilon})-59.47\right]_+ \qquad (6)$$

Provided that recrystallisation arises during multiple deformation steps, the portion of the retained strain ε must be specified and subtracted from the total strain. In this case, the austenite grain size D_γ means the recrystallised austenite grain size. The quantity in the

parentheses comes from the deformation bands, which are taken into account by Kvackaj only when the retained strain ε exceeds 0.475.

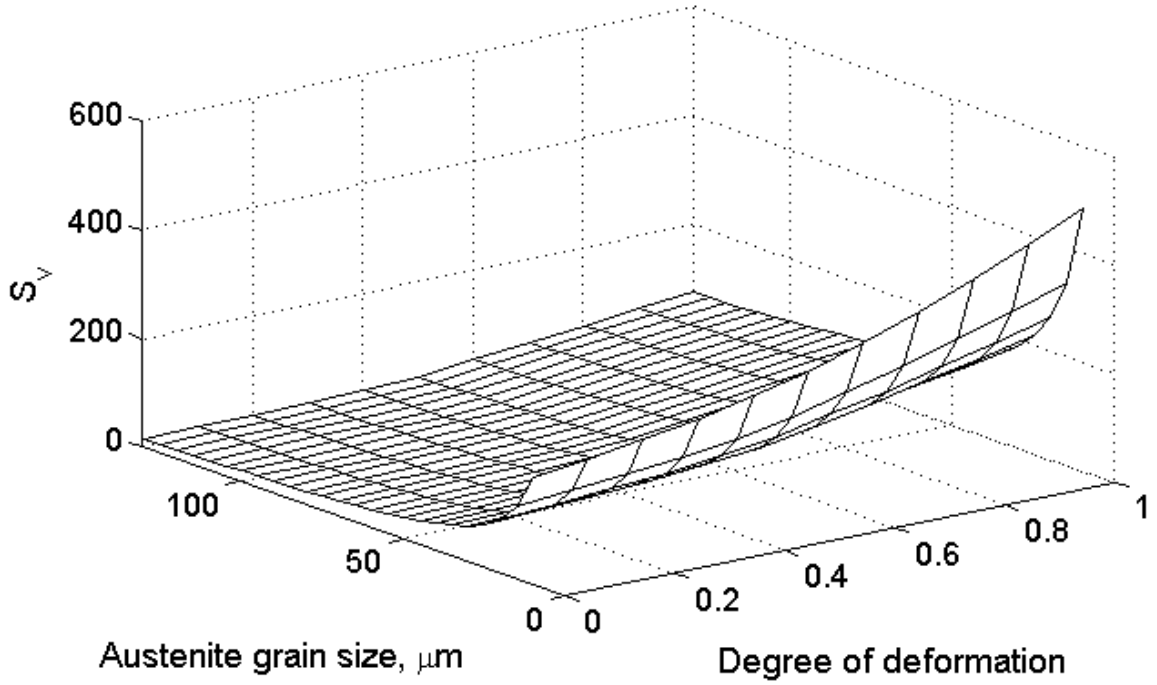

Figure 2: S_v function which represents the austenite conditioning as a function of austenite grain size D_γ and retained strain ε. The austenite grain size must be that after the repeated recrystallisation, which might take place during deformation.

The identification of the functions $g_{f1}(T)$ and $g_{f2}(D_\gamma,\varepsilon)$ in eqn. (1) as well as the coefficients τ_m and c_{KM} in (2), (4) from experimental data will be discussed later.

Experimental procedure

Physical process simulation. The process simulation of hot rolling for dual phase steel has been done in deformation dilatometer so that the rough process window can be addressed and the necessary experimental data on the effect of retained strain can be provided for the parameter identification of ferrite formation. Small cylindrical samples with a diameter of 5 mm and a height of 10 mm were prepared for hot compression tests in deformation dilatometer Baehr DIL-805A/D with thermomechanical cycle as described in **Figure 3**.

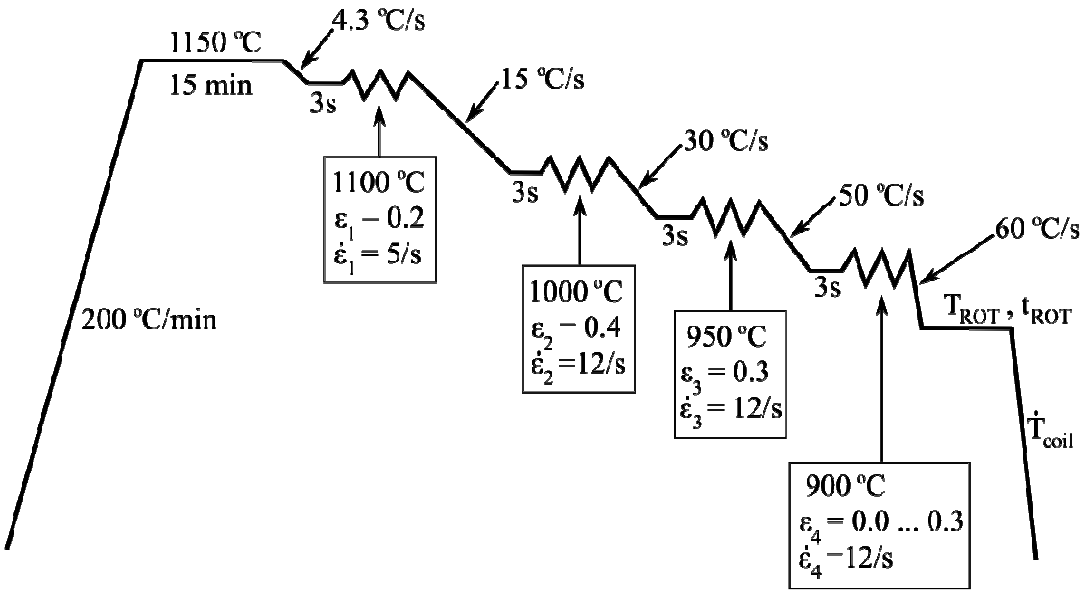

Figure 3: The thermomechanical cycle simulating hot rolling by means of dilatometer.

The samples were heated at 200°C/minute and austenitized at 1150 °C for 15 minutes. Four deformation steps were carried out at decreasing temperatures of 1100, 1000, 950, and 900°C, respectively. The process parameters varied only in the last deformation step, isothermal holding simulating ROT and the continuous cooling to coiling temperature. The degree of deformation in the last deformation, ε_4, ranged from 0.0 to 0.3. The holding time on ROT (t_{ROT}) varied between 0 and 9 s while holding at an isothermal temperature of 640 to 770°C. It has been done for different ferrite fraction resulting in different average carbon content in the remaining austenite. The cooling rate to coiling temperature $\dot{T}_{coil}$ was varied between 7 and 67 K/s. It should help to reveal the hardenability of the current dual phase steel.

The phase fraction was then analysed at the end of the thermal cycle in optical microscope by etching with nital as well as Le Pera reagent for the adequate differentiation between martensite and bainite. If possible, the metallographic analysis has been performed using automatic image analysis software AnalySIS®. A difficulty arises for the differentiation between bainite and martensite as well as between bainitic ferrite and polygonal bainite. In these cases, the phase fraction has been identified manually.

Experiment from prior austenite grain size. The initial austenite grain size after austenitization was investigated in small sheet samples with dimension of 7×4×1 mm by reheating the sample in the dilatometer to 1150 °C for 15 minutes, then quenching with the cooling rate as high as 600 K/s before annealing at 550 °C for 20 hours followed by etching with picric acid solution. However, the austenite grain size is subject to refinement due to the static recrystallisation which takes place during the following deformation steps. As the prior austenite grain boundaries are proved to be hardly visible in deformed samples, the analysis of recrystallised austenite grain size in this work employs the equation proposed by Sun et al. [7]

$$D_{rex} = BD_0^z \varepsilon^{-p} \exp\left(-\frac{Q_{gx}}{RT}\right) \tag{7}$$

where B = 100 $\mu m^{2/3}$, z = 1/3, p = 0.37 and Q_{gx} = 28 kJ/mole for 0.17 wt-% C steel. D_0 is the austenite grain size before recrystallisation and D_{rex} is the newly recrystallised austenite grain size. The application and the proof of this analysis have been done by double hit test as described in [5]. The newly recrystallised grain size must be recalculated for each deformation step.

Only the last deformation step was predicted to be under the recrystallisation stop temperature (T_{nr}), by employing the following empirical equation [8]:

$$T_{nr}(°C) = 887 + 464C + (6645Nb - 664\sqrt{Nb}) + (732V - 230\sqrt{V}) + 890Ti + 363Al - 357Si \quad (8)$$

This shows that the T_{nr} could be as high as 930°C, while the temperature in the last deformation step is 900 °C. Besides, according to the following high cooling rate applied to achieve the required isothermal temperature (T_{ROT}), the time allowed for static recrystallisation is shown to be extremely limited. The degree of deformation applied in this last deformation step is hence considered to be the retained strain.

Experimental Results

The initial austenite grain size after the austenitization in the cycle in **Figure 3** was measured to be 100 μm. As during all three first interpass time intervals, enough static recrystallisation was shown by double hit test, the recrystallised austenite grain size was therefore calculated by repeatedly applying eqn. (7) for all three deformation steps. The wording 'the recrystallised austenite grain size' from now on will mean the final recrystallised austenite grain size after the three first deformation steps and before entering the last deformation in non-recrystallisation zone. It was found to be 35 μm according to the cycle in **Figure 3**. It is the austenite grain size before entering the last deformation step, which is considered to be non-recrystallisation zone.

The ferrite fractions obtained from the same cycle with different varying process parameters on last deformation step and ROT are revealed in **Figure 4**, as the results of different retained strain ε as well as temperature and holding time on ROT (T_{ROT}, t_{ROT}). **Figure 4(a)** represents the ferrite fraction obtained from strain free austenite, while **Figure 4(b)** represents the effect of retained strain of 0.3. Both cases correspond to the austenite grain size of 35 μm. The ferrite transformation time varies from 0 to 10 s, while the holding temperature varies from 650 to 770 °C.

Note that the scattered experimental data of phase fraction arise on the one hand from the inaccuracy in the interpretation of the metallographs, generally of order ±5%. On the other hand, it is a result from the significant temperature overshooting in some samples during fast cooling down to the required isothermal temperature. The isothermal holding time stated in the diagram is therefore the time interval, during which the temperature deviation from the expected isothermal holding temperature was less than ±2%.

(a)

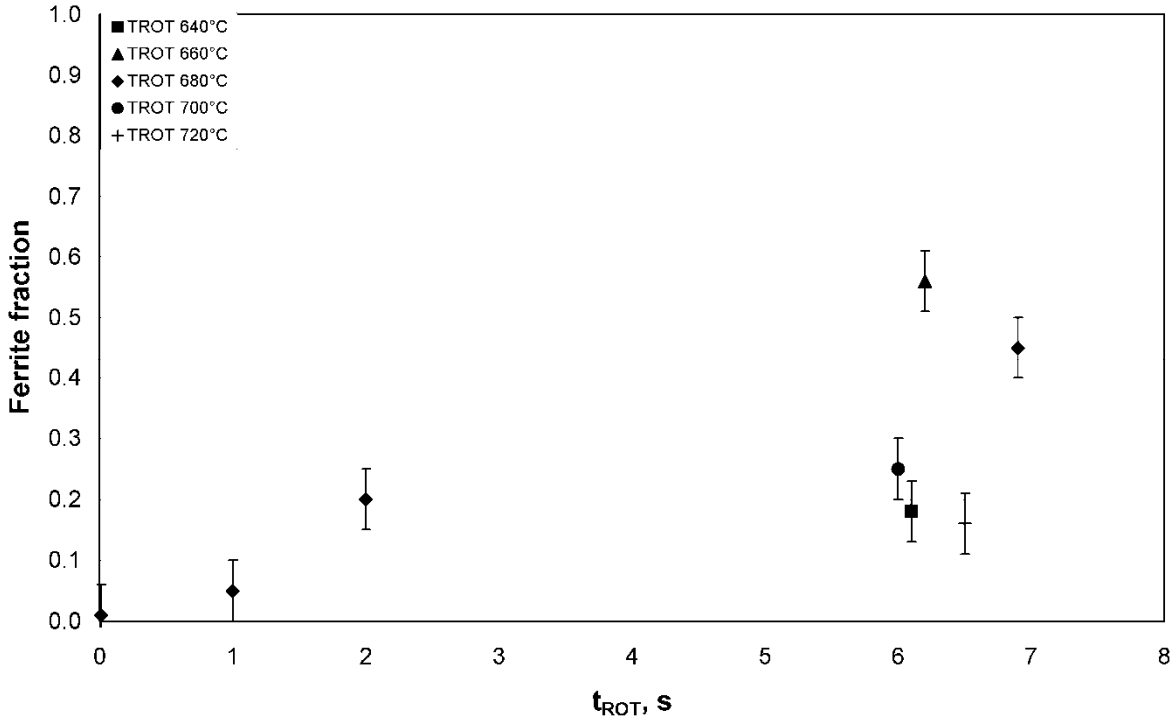

(b)

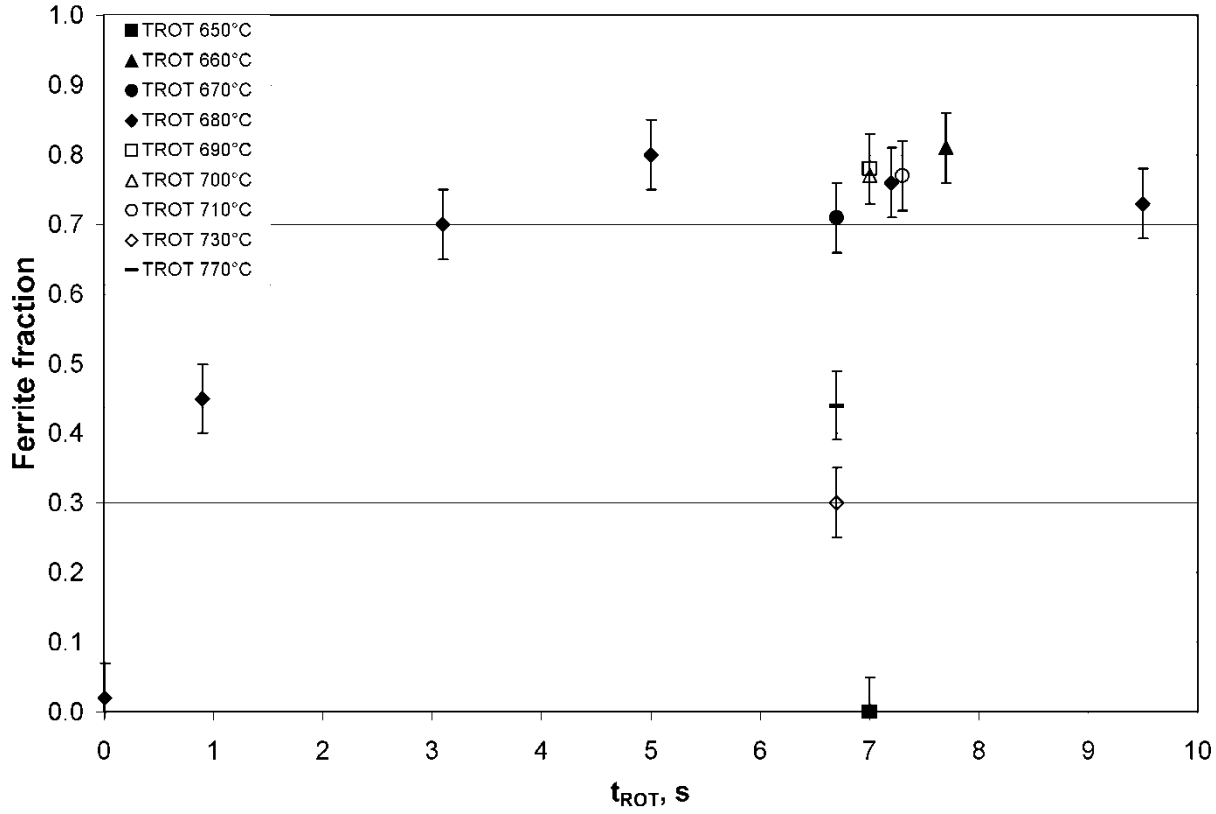

Figure 4: Ferrite fraction obtained by varying process parameters. The isothermal ferrite transformation time t_{ROT} ranges from 0 to 10 s and the holding temperature T_{ROT} varies from 650 to 770 °C. The recrystallised austenite grain size from former deformation step D_γ equals 35 µm; (a) retained strain $\varepsilon = 0.0$, (b) retained strain $\varepsilon = 0.3$.

The variation of the cooling rate $\dot{T}_{coil}$ after the ferrite formation in the process simulation in **Figure 3** can reveal the hardenability of the remaining austenite according to different degrees of carbon enrichment, which is proportional to the ferrite fraction. This can be roughly visualised by 'modified' CCT diagrams as shown in **Figure 5**. **Figure 5(a)** shows the hardenability of the remaining austenite with average carbon content of 0.2, after forming ferrite isothermally at 680 °C for 3 s and the ferrite fraction of 0.7 was formed. The four curves show the cooling profile of samples with different cooling rates varying from 7 to 60 K/s. These cooling rates were measured as an average from 600 to 200 °C.

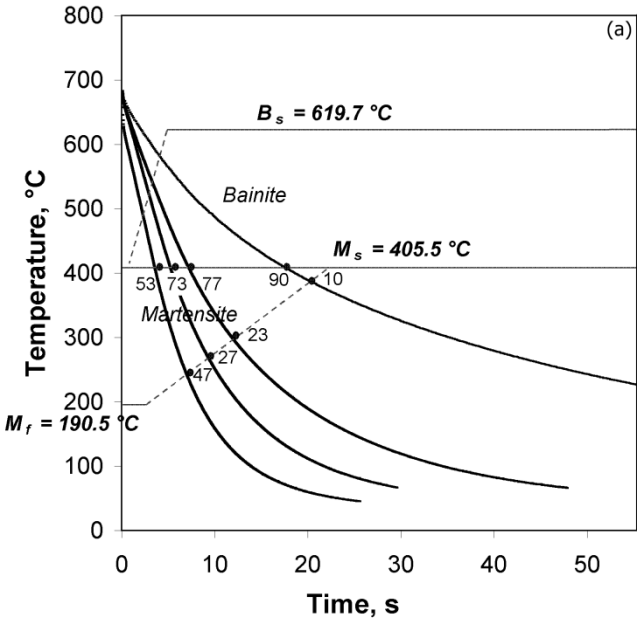

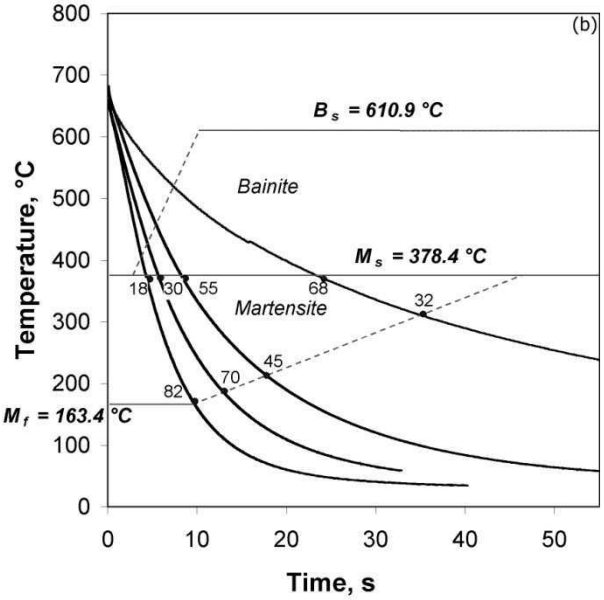

Figure 5: The modified CCT diagram from carbon enriched austenite. The curves represent the cooling profile of the samples, while the regions of bainite and martensite were drawn by using empirical equations for B_s, M_s, M_f , and the phase fraction analysis; (a) average carbon content of 0.2%, (b) average carbon content of 0.3%.

The bainite and martensite region must be estimated from the calculated temperatures of bainite start B_s, martensite start M_s, and martensite finish M_f, which were calculated from empirical equations proposed by Lee for B_s [9], Lorenz for M_s [4] (eqn. (5) shown in model description), and Petty for M_f [10], respectively, as shown below:

$$B_s = 745\text{-}110C\text{-}59Mn\text{-}39Ni\text{-}68Cr\text{-}106Mo+17MnNi+6(Cr)^2+29(Mo)^2 \quad (9)$$

$$M_s = 506.6 - 338.7C - 18.3Mn - 14.5Cr + 1.3Si \quad (10)$$

$$M_f = M_s - 215. \quad (11)$$

This is because the fraction of bainite and martensite is relatively small compared to the volume of the whole sample, in total as small as 0.3 in this case, and results in a really weak dilatation signal.

The nose of the bainite region and the latter part of the martensite region could be suggested by the fraction of bainite and martensite, which are stated at the end of their phase regions. It has to be noted that only the remaining austenite is being considered and therefore rescaled to be 1.0. The fraction of the bainite and martensite discussed in this diagram are calculated from this portion. The higher the bainite fraction obtained in the sample, the deeper is the cooling curve of the sample in the bainite region. The distance between the bainite nose (dashed line) and the M_s temperature along the cooling line of each sample is therefore proportional to the bainite fraction. Constructing the martensite region follows the same approach. In this case, the less the martensite fraction, the higher is the M_f temperature. A good reasoning is that the higher fraction of bainite results in more carbide precipitation. Consequently, less carbon enrichment remains in the austenite. This corresponds to the literature [11] showing the increase in the temperature interval M_s-M_f with carbon content from 0-0.6%.

The shift of these critical temperatures as well as of the bainite and martensite nose due to the higher carbon enrichment can be seen in **Figure 5(b)**. The austenite in this case has the carbon enrichment of 0.3% after forming ferrite at 680 °C for 5 s for a ferrite fraction of 0.8. The bainite region was shifted to the right hand side and the critical cooling rate to avoid bainite is decreased.

Parameter identification for the rate law model

To identify the data functions for the growth of ferrite at first an isothermal experiment is considered. Assuming that the retained strain is zero, i.e., $\varepsilon = 0$, one can conclude that

$$g_{f2}(D_\gamma, \varepsilon) = 1.$$

For a particular temperature T the function $g_{f1}(T)$ can be identified from eqn. (1) as follows:

$$g_{f1}(T) = \frac{\ln \dfrac{f_{eq} - f(t_S)}{f_{eq} - f(t_E)}}{t_E - t_S}. \quad (12)$$

Here, t_S stands for the time, when the transformation starts, while t_E stands for the time when it ends. To derive $g_{f1}(T)$ over a range of temperatures, several data sets $(t_E, f(t_E))$ with measured isothermally transformed ferrite fractions and corresponding transformation times for varying transformation temperatures have to be given. The equilibrium volume fraction of ferrite f_{eq} can be predicted by the thermodynamic calculation software ThermoCalc^{TM}.

The results of the identification of the function $g_{f1}(T)$ are shown in **Figure 6**.

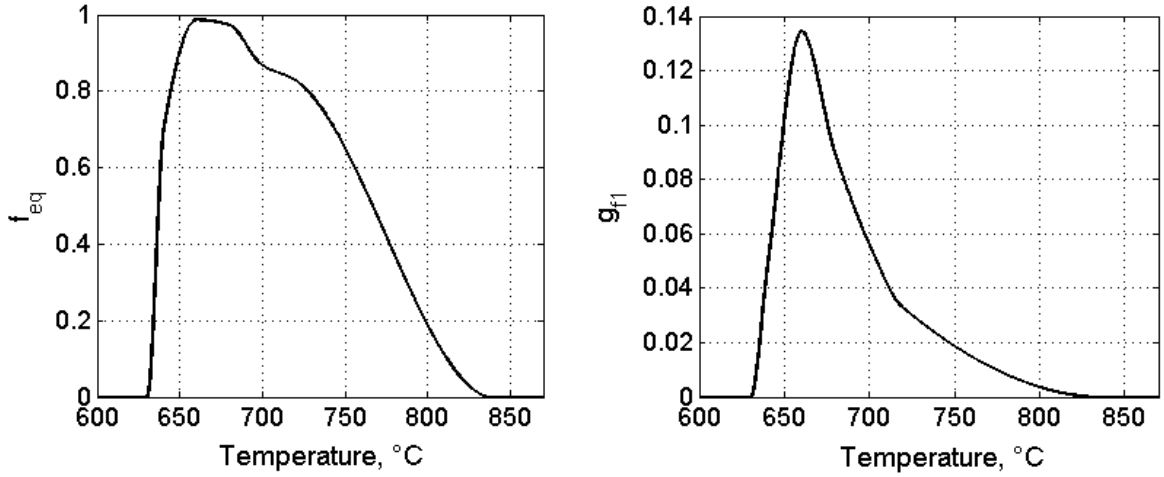

Figure 6: Equilibrium ferrite fraction f_{eq} (T) computed with ThermoCalc™ and the function $g_{f1}(T)$ computed from eqn. (12)

Using dilatometer results for the case of fast cooling, where only martensite is produced, one can obtain the parameters c_{KM} and τ in eqn. (4) in a straightforward way as

$$c_{KM} = 0{,}0214$$
$$\tau = 0.67 .$$

An essential part of the parameter identification is a fitting of the function $g_{f2}(D_\gamma, \varepsilon)$ in eqn. (1). This factor describes the influence of austenite grain size and retained strain coupled in the function S_v on the ferrite transformation. The simplest choice for $g_{f2}(D_\gamma, \varepsilon)$ is to assume a linear relationship on S_v, i.e.

$$g_{f2}(D_\gamma, \varepsilon) = \alpha_1 S_v(D_\gamma, \varepsilon) + \alpha_2 \ , \qquad (13)$$

where S_v is calculated from (6) and the parameters α_1, α_2 have to be fitted to the experimental data.

It should be noted that a fitting of the function $g_{f2}(D_\gamma, \varepsilon)$ is carried out for the austenite grain size $D_\gamma = 35\ \mu m$ according to the experimental data from the former section. Moreover, for vanishing retained strain, i.e. $\varepsilon = 0$, $g_{f2}(D_\gamma, \varepsilon)$ has to satisfy

$$g_{f2}(35{,}0) = 1 .$$

Since in this case $S_v(35{,}0) = 57.14$ it follows immediately from (11) that $\alpha_2 = 1 - \alpha_1 \cdot 57{,}14$. To estimate the unknown parameter value α_1 from the given experimental data set $(T^i_{ROT}, t_{ROT}, \hat{f}_i)$, $i = 1,..., l$, the least squares function

$$J(\alpha_1) = \sum_{i=1}^{l} (f_i(t_{ROT}, \alpha_1) - \hat{f}_i)^2$$

is minimized under the constraint

$$\dot{f}(t) = \left[f_{eq} - f \right]_+ g_{f1}(T_{ROT})(\alpha_1 \cdot S_v(35{,}0.3) - \alpha_1 \cdot 57.14 + 1), \quad t \in (0, t_{ROT})$$
$$f(0) = 0$$

To solve the optimization problem formulated above the MATLAB optimization toolbox was used. The obtained optimal solution is $\alpha_1^* = 0.2174$.

Simulation results

Using a MATLAB ODE solver, the phase transformation kinetics of ferrite and martensite can be computed as a function of the related process parameters, namely, austenite conditioning (step 1 in **Figure 1**), isothermal holding time and temperature (step 3 in **Figure 1**) as well as the final cooling (step 4 in **Figure 1**).
An example is depicted in **Figure 7,** where the development of phases is shown along the processing time and temperature profile and compared with those derived at the end of dilatometer experiment. It simulates the transformation from austenite deformed with strain of 0.3. The dashed line shows the temperatur profile taken from the experiment.

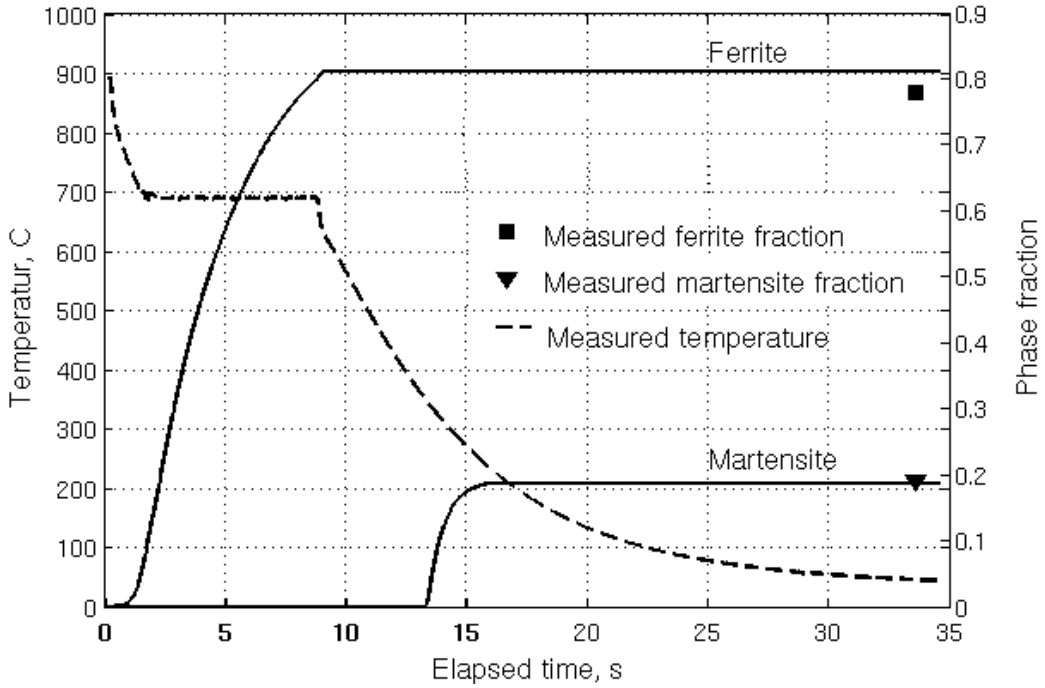

Figure 7: Simulated evolution of phase fractions along the processing time and measured temperature profile, in comparison with the measured phase fraction at the end of the dilatometer experiment. The elapsed time starts from the beginning of ROT. Retained strain is 0.3, holding temperature 690 °C and holding time 7 s. The average cooling rate in the following step, measured from 600 to 200 °C is 61K/s.

The transformation shown here starts after 1 s of the simulated process on ROT, at 690°C. After the time interval of 7.85 s, which includes the holding time on ROT $t_{ROT} = 7\,\text{s}$, the ferrite fraction reaches 0.81. The next cooling region simulates the cooling step to coiling temperature (step 4 in **Figure 1**), in this case with the average cooling rate of 61 K/s, measured from 600°C down to 200°C. When the temperature reaches the martensite start temperature M_s, which was calculated to be 351.3°C according to the carbon enrichment from the corresponding simulated ferrite fraction, martensite starts to form and then finishes at 267.7 °C with the phase fraction of 0.19. The phase fraction analysed from the dilatometer sample is revealed to be as follows: ferrite 0.78, bainite 0.03 and martensite 0.19. The numerical simulation results are in a good agreement to the measured ferrite and martensite

fractions. The deviation of the simulated ferrite fraction from the experimental one is less then 4%.

The available experimental data of transformed ferrite fractions for different holding temperatures on ROT and holding time $t_{ROT} = 7s$ presented in the previous section in **Figure 4** have been compared with the ones calculated from the rate law model. The results of this model validation are shown in **Figure 8.**

In view of the scattering of experimental data the qualitative agreement is quite good. Some deviations of the predicted phase fractions from the measurements arise from the fact that the holding time on ROT, which should be 7s, cannot be reached exactly during each experiment. However, one should remark that further experimental studies with different values of retained strain are necessary for a more reliable parameter identification.

Additionally, the isothermal ferrite growth has been simulated during the holding time on ROT, $t_{ROT} = 7\,s$, with holding temperature $T_{ROT} = 680°C$ and for two different retained strains, $\varepsilon = 0$ and $\varepsilon = 0.3$. The simulation results and experimental data are compared in **Figure 9**. It shows very good agreement between calculated and measured ferrite fractions for the degree of deformation $\varepsilon = 0$ (dashed line). The prediction of the ferrite transformation in the case of the degree of deformation of 0.3 shows deviations from the experimental values for the early transformation stages. The reason for the big deviation of the simulation result from the measurement for the end time t = 7s is an inaccuracy in experimental data, which shows a decreasing growth of ferrite fraction at this time instant.

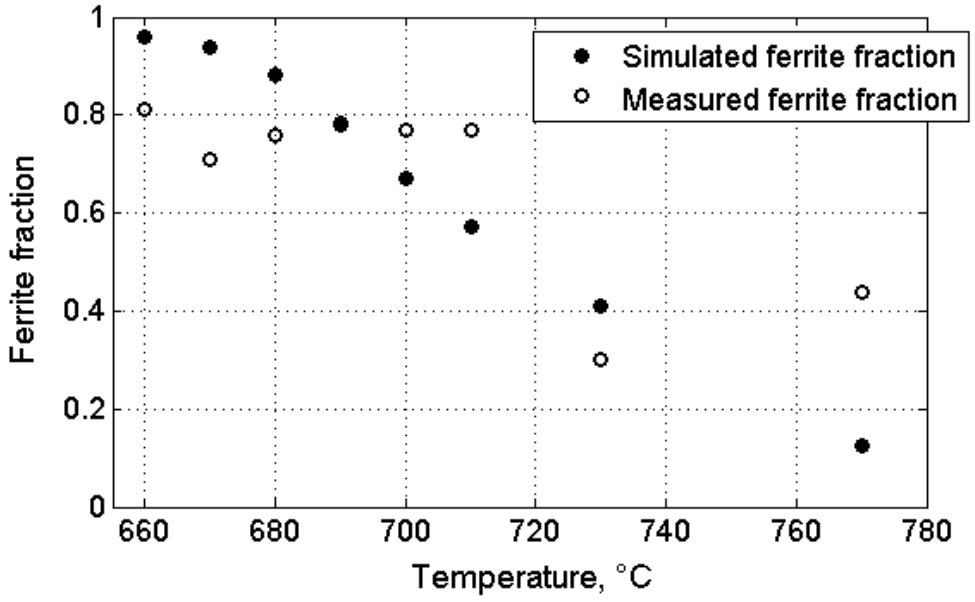

Figure 8: A comparison between the simulated and measured transformed ferrite fraction for different holding temperatures on ROT and degree of deformation $\varepsilon = 0.3$. The holding time on ROT is 7s.

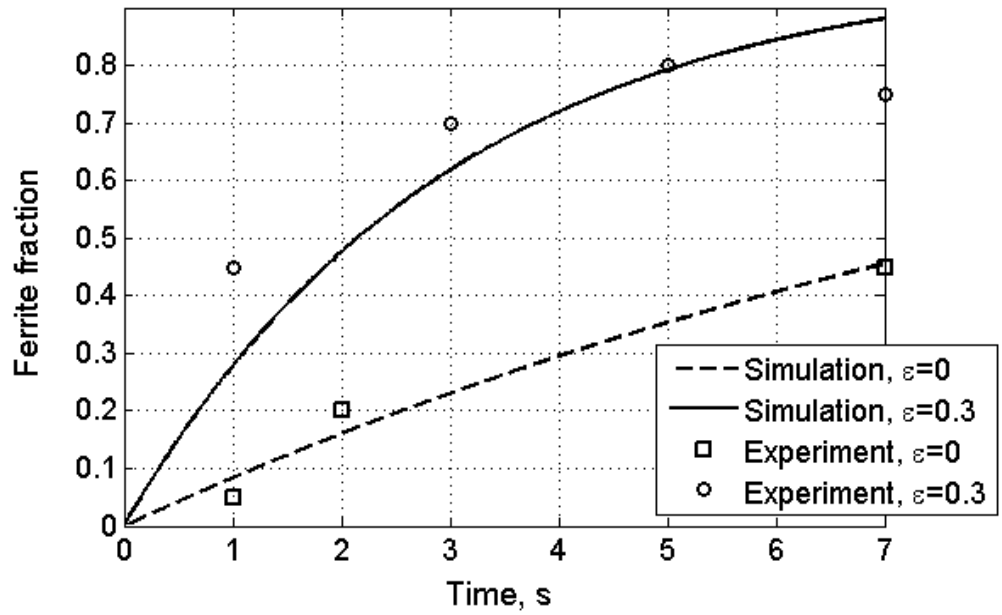

Figure 9: comparison between the simulated and measured ferrite fraction for T_{ROT} = 680°C.

Numerical process design

The most important process parameters influencing the final phase mixture are the holding time and temperature as well as the degree of deformation. For a better process understanding a systematic parameter study has been performed, whose results are depicted in the following Figures. **Figure 10** shows the resulting ferrite fraction as a function of degree of deformation and of holding temperature for holding times of 5s, 7s and 9s, respectively. **Figure 11** depicts the ferrite fraction as a function of holding time and temperature for degrees of deformation of 0, 0.2 and 0.3, respectively.

(a)

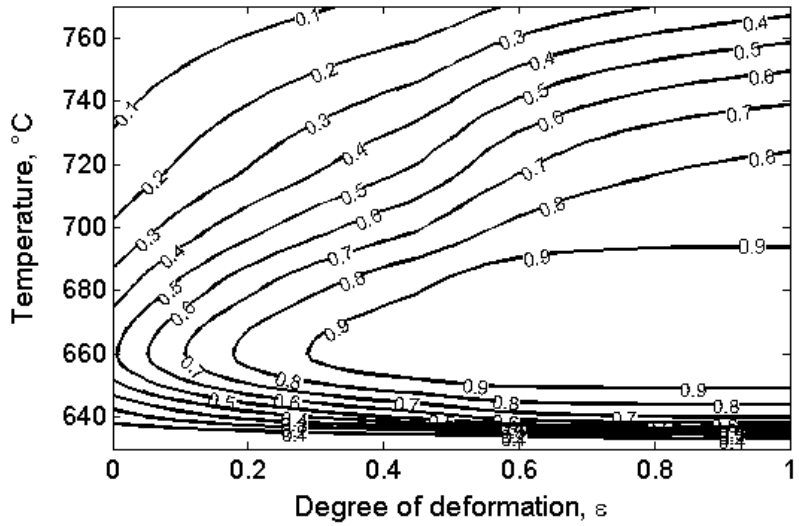

(b)

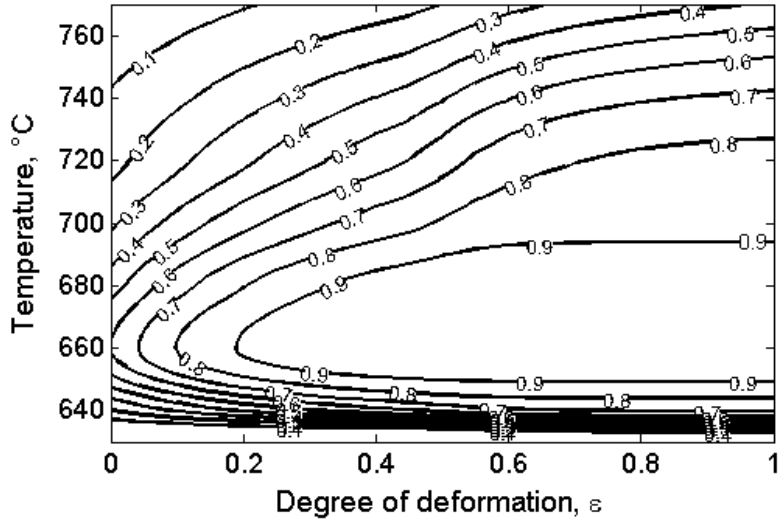

(c)

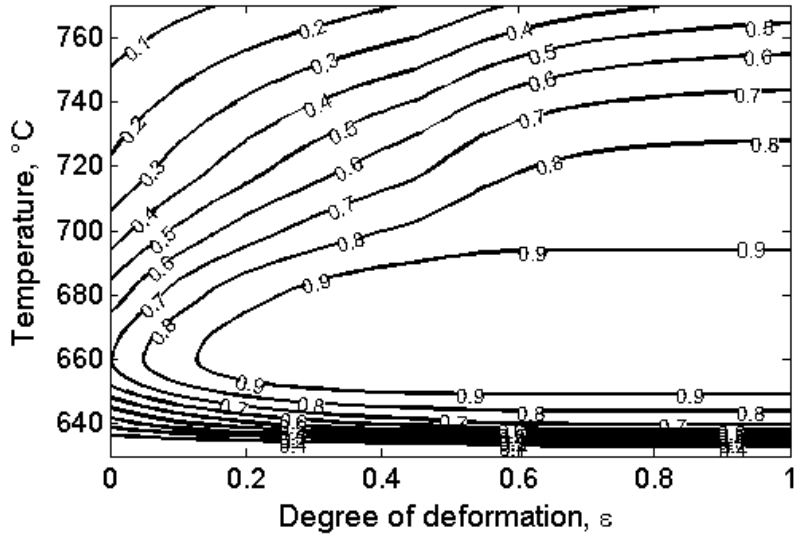

Figure 10: Contours of the simulated transformed ferrite fraction represented as a function of different retained strains and holding temperatures on ROT for holding times of 5s (a),7s (b), 9s (c), respectively. The contour lines characterize the process parameters deformation degree and isothermal holding temperature, where for a prescribed holding time the marked fraction of ferrite has been reached.

(a)

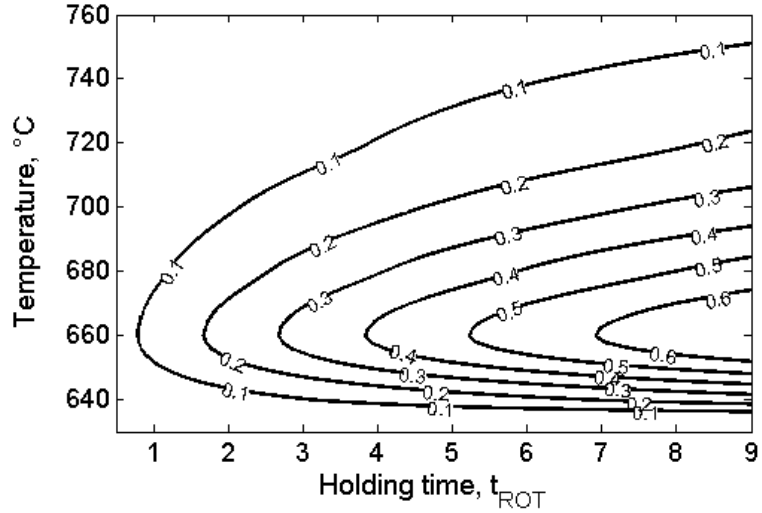

(b)

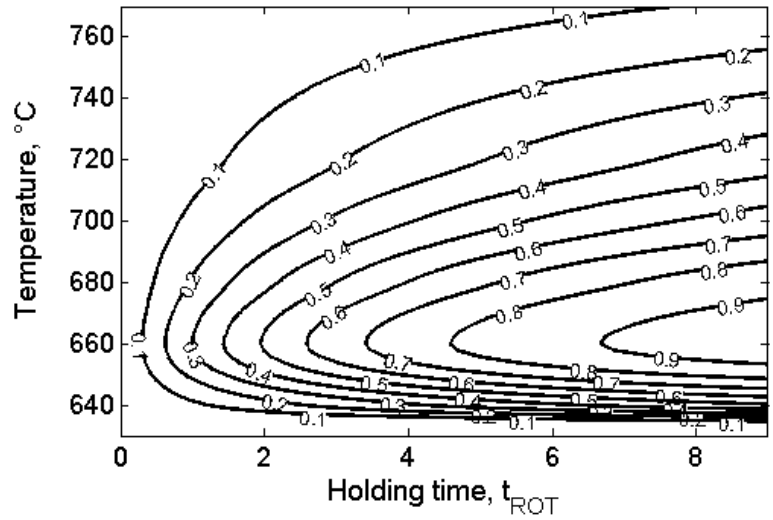

(c)

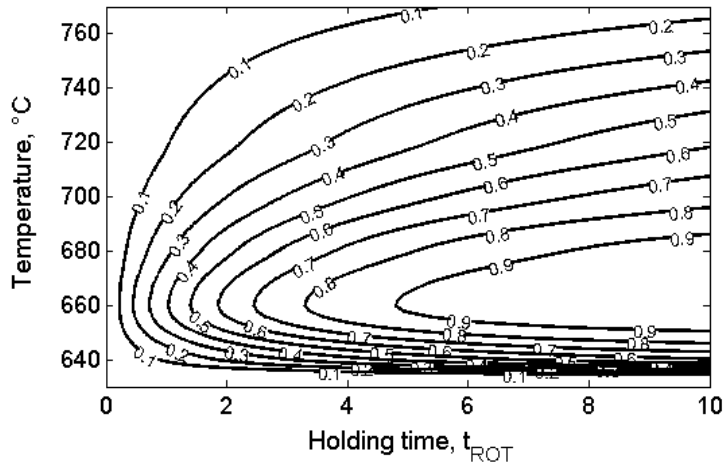

Figure 11: Contours of the simulated transformed ferrite fraction represented as a function of different holding times and temperatures on ROT for retained strains (a) $\varepsilon = 0$, (b) $\varepsilon = 0.2$, (c) $\varepsilon = 0.3$, respectively. The lines characterize the process parameters holding time and isothermal holding temperature where for a prescribed deformation degree ε the marked amount of ferrite is reached.

As for the process discussed in this paper the final ferrite fraction after coiling is a function of three process parameters ε (degree of last deformation), T_{ROT} (isothermal holding temperature on ROT) and t_{ROT} (isothermal holding time on ROT), respectively, the results are plotted as isothermal contour plots for one fixed parameter and two free parameters on the axes.
Holding in mind that a proper dual-phase steel consists of approximately 80 % ferrite those process parameters have to be identified, where this fraction can be reached. Aiming at a robust process it is important to have a look at the gradient in the contour plot. **Figure 10** shows that for all isotheral holding times there is a process window between 720 and 740 °C and between 0.6 and 1.0 deformation, where the ferrite fraction stays remarkably constant. On the other hand, **Figure 11** shows that for a holding time of 0 s the desired ferrite fraction will not be achieved within 9 s holding time, but for higher holding times there is a stable process window in terms of holding time at 640 °C.

Conclusion and outlook

Rate equations for ferrite and martensite formation have been employed to describe the phase transformation in hot rolled dual phase steels as functions of process parameters such as austenite conditioning, holding condition on the ROT and the cooling to coiling procedure. The experimental process simulation was carried out in hot deformation dilatometer for the rough process window and for the quantities required for parameter identification. The simulation results were validated with those derived from the process. A detailed parameter study allowed for the determination of a stable process window to obtain the desired phase distribution for dual phase steel. In a forthcoming paper it will be shown how the results of process simulation and numerical simulation using the rate law model can be utilized for the design of a real hot rolling mill. Here, the computation of the most proper process parameters by means of optimal control theory will play an important role [12,13].

Another direction of future research is the appropriate modelling of bainitic growth. An important issue will be to account for a possibly inhomogeneous carbon enrichment in the remaining austenite, since the carbon distribution profile in the remaining austenite generally shows higher concentration in the region near the α/γ interface due to the limited diffusivity in austenite. Provided that this inhomogeneity has been proven to result in significantly different bainite and martensite phase fractions from taking the average carbon content, it would be challenging to include this effect in the model as a ‘fine tuning’.

References

[1] Bleck, W.: Multiphase steels for car bodies, Modern Developments in Metallurgy and Technologies of Steels for Automotive Industry, International Seminar, Proceedings, 16.-19.02.2004, Moskau, Russland. Moskau: TSNII Chermet 2004, pp. 112-127.

[2] Hömberg, D.; Weiss, W.: PID Control of Laser Surface Hardening of Steel, IEEE Transactions on control systems technology 14 (2006), pp. 896-904

[3] Koistinen, D.; Marburger, R.: A general equation prescribing the extent of the austenite-martensite transformation in pure iron-carbon alloys and plain carbon steels, Acta Met. 7 (1959), pp. 59–60.

[4] Lorenz, U.: Anwendung von Werkstoffmodellen auf die Phasenumwandlung und die Austenitkonditionierung von Stählen, Dissertation, RWTH Aachen, 2003.

[5] Suwanpinij, P.; Mukherjee, K.; Graf, M.; Prahl, U.; Bleck, W.; Kawalla, R.: Modelling of phase transformation and mechanical properties in hot rolled steels, Proceeding of TMS 2010, 14.-18.02.2010, Seattle, Washington, USA (2010), CD.
[6] Kvačkaj, T.; Mamuzic, I.: ISIJ Int. 38 (1998), 11, p. 1270.
[7] Sun, W.B.; Militzer, M.; Hawbolt, E.B.; Meadowcroft, T.R.: Trans. ISS (1998) 5, pp. 85-94.
[8] Boratto, F.; Yue, S.; Jonas, J.J.; Lawrence, T.H.: Design of schedules for the production of high strength microalloyed steel strip in a hot steckel mill, Proc. Thermec'88 (ed.), I. Tamura (Tokyo: Iron and Steel Inst.), (1988), p. 383.
[9] Lee, Y.-K.: Journal of Materials Science Letters (2002), p. 1253.
[10] Petty, E.R.: Martensite Fundamentals and Technology, Petty, E.R. (Ed.). London: Longman, 1970, p. 2.
[11] Zimmermann, R.; Günther, K.: Metallurgie und Werkstofftechnik, Band 1, Deutscher Verlag für Grundstoffindustrie, Leipzig, GDR, p. 271.
[12] Hömberg, D.; Volkwein, S.: Control of laser surface hardening by a reduced-order approach using proper orthogonal decomposition, Math. Comput. Modelling, 38 (2003), pp. 1003–1028.
[13] Hömberg, D.; Kern, D.: The heat treatment of steel – a mathematical control problem, Mat.-wiss. u. Werkstofftech. 40 (2009), pp. 439-442.